Rice

RESEARCH Open Access

OsPRDA1 Interacts With OsFSD2 To Promote Chloroplast Development by Regulating Chloroplast Gene Expression in Rice

Chao Zhang[1], Lengjing Wang[1], Zirui Wang[1], Qiang Dai[1], Haiyang Feng[1], Shu Xu[1], Xueju Liu[1], Jiaqi Tang[1] and Hengxiu Yu[1*]

Abstract
Chloroplasts are vital for photosynthesis, and their development necessitates proper expression of chloroplast genes. However, the regulatory mechanisms underlying rice chloroplast gene expression have not been fully elucidated. In this study, we obtained an albino mutant of rice, *white seedling and lethal 1* (*wsl1*), which displays significantly decreased chlorophyll contents and impaired chloroplast ultrastructure. The causal gene *Oryza sativa PEP-RELATED DEVELOPMENT ARRESTED 1* (*OsPRDA1*) was isolated using Mutmap + and verified by gene editing and complementary assays. The expression of *OsPRDA1* is induced by light, and OsPRDA1 is localized in chloroplasts. Transcription sequencing revealed that genes related to photosynthesis were differentially expressed in *wsl1*. The expression levels of the examined plastid-encoded RNA polymerase (PEP)-dependent chloroplast genes are downregulated due to the mutation of *OsPRDA1*. Moreover, OsPRDA1 interacts with OsFSD2, a member of PEP-associated proteins (PAPs). Knockout of *OsFSD2* leads to the albino and seedling-lethal phenotype and downregulation of PEP-dependent chloroplast genes. Together, our results demonstrated that OsPRDA1 plays essential roles in rice chloroplast development, probably by facilitating the function of the PAP complex and chloroplast gene expression.

Keywords OsPRDA1, OsFSD2, Chloroplast Gene Expression, Chloroplast Development, PAPs

Background

Chloroplasts are semiautonomous organelles that contain DNA and gene expression apparatuses (Martin et al. 1998). The chloroplast genomes of most land plants encode approximately 110–130 genes (Daniell et al. 2021). These genes are transcribed, according to their promoter specificity, by two types of RNA polymerase: nuclear-encoded RNA polymerase (NEP) and plastid-encoded RNA polymerase (PEP) (Hedtke et al. 2000; Swiatecka-Hagenbruch et al. 2008; Börner et al. 2015). The single-subunit RNA polymerase NEP is encoded in the nuclear genome and is responsible for transcribing genes encoding PEP subunits and other housekeeping genes (Yu et al. 2014a, b). PEP, encoded by the chloroplast genes *rpoA*, *rpoB*, *rpoC1*, and *rpoC2*, plays an essential role during chloroplast biogenesis from proplastids and functions as the predominant RNA polymerase in mature chloroplasts (Zhelyazkova et al. 2012).

The PEP-centered transcription apparatus is assembled from the PEP core (2α, β, β'1, and β'2) and more than a

*Correspondence:
Hengxiu Yu
hxyu@yzu.edu.cn
[1]Jiangsu Key Laboratory of Crop Genomics and Molecular Breeding/Zhongshan Biological Breeding Laboratory/Key Laboratory of Plant Functional Genomics of the Ministry of Education/Jiangsu Co-Innovation Center for Modern Production Technology of Grain Crops, Agricultural College of Yangzhou University, Yangzhou 225009, China

dozen nuclear-encoded PEP-associated proteins (PAPs) (Pfannschmidt et al. 2015). Recently, the Cryo-EM structures of the plant plastid-encoded RNA polymerase were determined (Wu et al. 2024). Fourteen PAPs located at the periphery of the PEP core were identified. Based on the locations and potential functions of the PAPs, they are grouped into four modules: the scaffold module (PAP1, PAP3, PAP5, PAP7, PAP8, PAP11, and PAP14), the RNA module (PAP2), the protection module (PAP4 and PAP9), and the regulation module (PAP6, PAP10^{I}, PAP10^{II}, and PAP13). *Arabidopsis* plants with mutations in PAP-encoding genes, with the exception of the newly identified *PAP14* gene, present defects in the PEP-mediated transcription of chloroplast genes and chloroplast development (Pfalz et al. 2006; Garcia et al. 2008; Myouga et al. 2008; Arsova et al. 2010; Steiner et al. 2011; Gilkerson et al. 2012; Yagi et al. 2012; Yu et al. 2013). Similarly, certain rice PAP homologs have been functionally characterized through chlorosis mutants (Wang et al. 2016a, b, 2021a, b; Lv et al. 2017; He et al. 2018; Lin et al. 2018; Qiu et al. 2018; Seo et al. 2024). In particular, PAP4 and PAP9, also known as FE SUPEROXIDE DISMUTASE3 (FSD3) and FE SUPEROXIDE DISMUTASE2 (FSD2), respectively, form a heteromeric protein complex and defend chloroplast nucleoids against oxidative stress. The *fsd2 fsd3* double mutant presents a severe albino phenotype, whereas the *fsd2* and *fsd3* single knockout mutants present pale green phenotypes (Myouga et al. 2008). Mutation of *ALM1*, the rice homolog of *FSD3*, results in the accumulation of excessive reactive oxygen and leads to seedling lethality. The overexpression of *ALM1* increased SOD enzyme activities, led to increased scavenging of superoxide anion radical (O_2^-) and conferred drought stress tolerance in rice seedlings (Wang et al. 2021b).

In addition to PAPs, other nuclear-encoded proteins also play roles in PEP-mediated plastid RNA transcription. The *AtECB1/MRL7* knockout lines presented an albino phenotype and decreased transcript levels of PEP-dependent plastid genes. Although AtECB1 was not identified in the PEP complex, it can interact with Trx Z and FSD3 (Qiao et al. 2011; Yu et al. 2014a, b). The *prin2* mutant of *Arabidopsis* presented lower expression levels of genes transcribed by PEP and impaired high light-dependent plastid redox signaling to the nucleus (Kindgren et al. 2012; Díaz et al. 2018). PRDA1, a chloroplast nucleoid protein, is required for early chloroplast development and is involved in the regulation of plastid gene expression in *Arabidopsis*. Moreover, PRDA1 interacts with FSD2 and AtECB1/MRL7, suggesting that PRDA1 probably acts as a component of the PEP complex and might be involved in the redox control of plastid gene expression (Qiao et al. 2014).

Despite extensive studies on the molecular mechanisms of chloroplast gene expression and development in *Arabidopsis*, identified players in rice are relatively rare. In this study, we cloned the *OsPRDA1* gene from the *white seedling and lethal 1* (*wsl1*) mutant and demonstrated that OsPRDA1 plays an essential role in rice chloroplast development, probably by facilitating the function of the PAP complex and chloroplast gene expression.

Results

Characterization of the *White Seedling and Lethal 1* Mutant

We obtained a rice mutant line segregating albino seedlings from our mutant library induced by ^{60}Co-γ-ray irradiation. This mutant presents white leaves from the emergence of the first leaf (Fig. 1A). With growth and development, the mutants consistently present white leaves and gradually wilt and die within three weeks (Fig. 1B, C). We designated this mutant *white seedling and lethal 1* (*wsl1*). The phenotype of *wsl1* is steadily inherited for several generations.

Albino phenotype is generally an indication of photosynthesis pigment deficiency. We measured and compared the photosynthetic pigment contents of ten-day-old wild-type and *wsl1* seedlings. Compared with the wild type, *wsl1* contained significantly less chlorophyll a (0.45 ± 0.00039 mg/g in the wild type and 0.043 ± 0.0047 mg/g in *wsl1*), chlorophyll b (0.20 ± 0.0057 mg/g in the wild type and 0.078 ± 0.0076 mg/g in *wsl1*), and carotenoids (0.20 ± 0.00049 mg/g in the wild type and 0.022 ± 0.0018 mg/g in *wsl1*) (Fig. 1D).

Chloroplast Development Is Impaired in *wsl1*

To investigate chloroplast development in *wsl1*, we compared the ultrastructure of chloroplasts in leaves from wild-type and *wsl1* plants by transmission electron microscopy (TEM) (Fig. 2). In the wild type, fully developed chloroplasts with massive thylakoid membranes and starch granules were observed. In contrast, the chloroplast morphology of *wsl1* was less organized. No thylakoid membranes or starch granules were observed in *wsl1* chloroplasts. Instead, there many oval-shaped vesicles were noted in the *wsl1* chloroplasts. Moreover, many densely stained globular structures, probably plastoglobules, were frequently observed in *wsl1* chloroplasts. These results indicated that the development of chloroplasts is impaired in *wsl1* plants.

Identification and Characterization of the Causal Gene *OsPRDA1*

A segregating population presented a 3:1 (177:48, $\chi^2_{(1)} = 1.61$, $P > 0.05$) segregation ratio between wild-type plants and mutants, indicating that the mutant phenotype was caused by a single recessive mutation

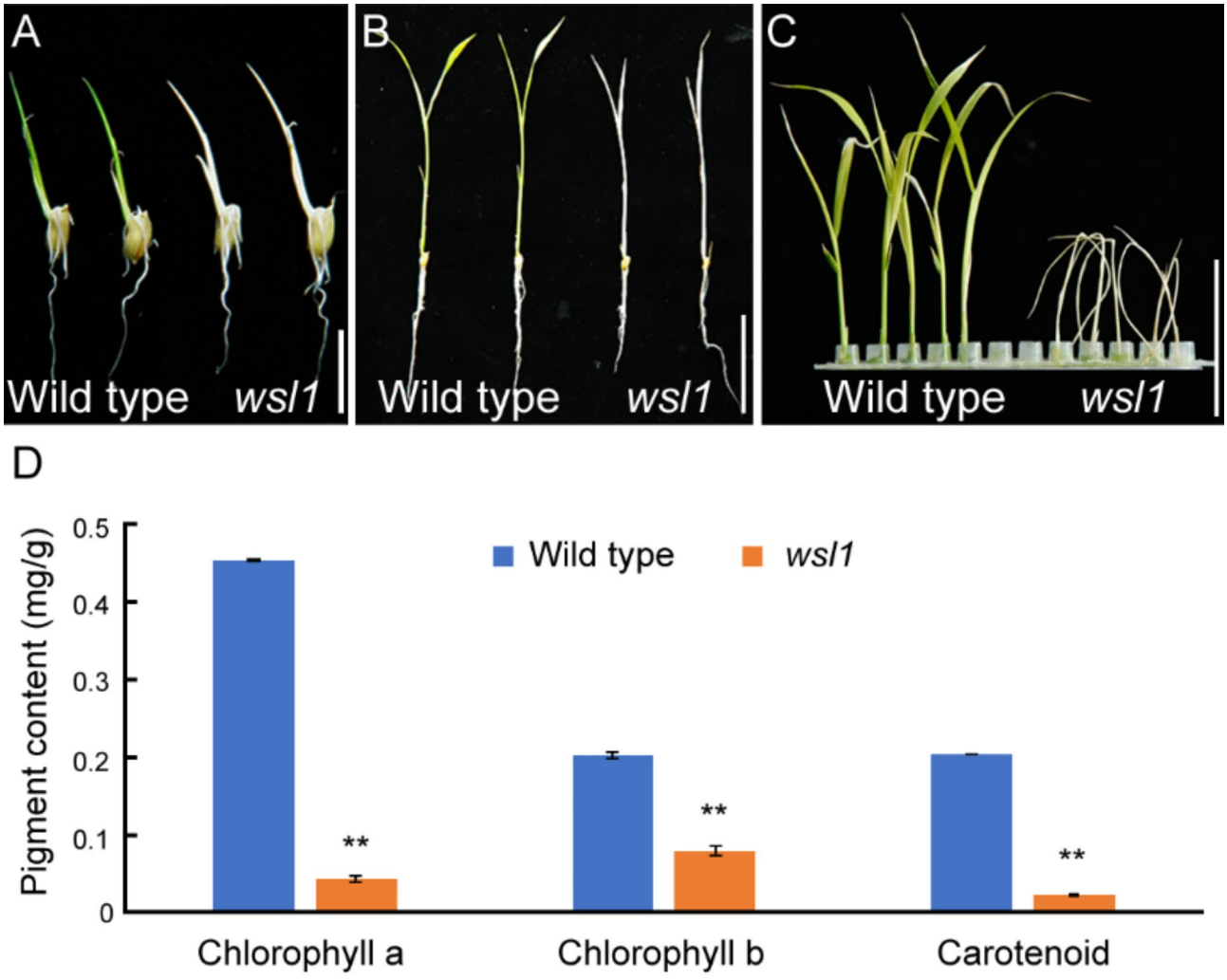

Fig. 1 Phenotypic characterization of *wsl1*
(**A-C**) Comparison of wild-type and *wsl1* seedlings at 3, 12, and 19 days after germination (DAG). Scale bars = 1 cm in A, 5 cm in **B** and **C**. (**D**) Photosynthetic pigment content in ten-day-old wild-type and *wsl1* seedlings. Data are presented as the mean ± SD. Asterisks indicate significant differences according to a two-tailed Student's *t* test (**$P < 0.01$)

in a nuclear gene. The causal gene was isolated by Mutmap + combined with the mutation filtering process we described previously (Fekih et al. 2013; Zhang et al. 2023). Only one 12-bp deletion (located at chr11-13462908 bp), with mutation indices of 1 (13/13) and 0.21 (3/14) in the mutant bulk and wild-type bulk, respectively, was identified. To verify the results of Mutmap + and our mutation filtration process, we sequenced 20 randomly selected seedlings from the segregating population using Sanger sequencing. As expected, the phenotype cosegregated with the genotype. All the mutants presented homologous mutation of the candidate deletion, and the seedlings without the mutant phenotype were a combination of the wild-type sequence and heterozygotes.

According to the Rice Genome Annotation Project, the candidate mutation is located in the fourth exon of the LOC_Os11g23790 gene. LOC_Os11g23790 is annotated as a coding gene of an expressed protein that shows similarity (74% identities and 88% positives) with *Arabidopsis* PEP-RELATED DEVELOPMENT ARRESTED 1 (PRDA1) (Qiao et al. 2014). Therefore, we designated this gene *OsPRDA1*. *OsPRDA1* consists of 9 exons. The open reading frame (ORF) is 1149 bp in length, and the deduced protein contains 382 amino acids. Mutation of *OsPRDA1* in *wsl1* results in a putative 4-amino acid deletion (residues 218–221) (Fig. 3A).

OsPRDA1 belongs to the protein family IPR038961, which is widely distributed within the plant kingdom. Interestingly, members of this protein family are present in specific bacterial species (such as *Anaerolineae bacterium*). Phylogenetic analysis revealed that plant PRDA1 homologs from monocots and dicots are clearly divided. Gymnosperms and bryophytes constitute isolated branches in the phylogenetic tree (Fig. 3B). Notably,

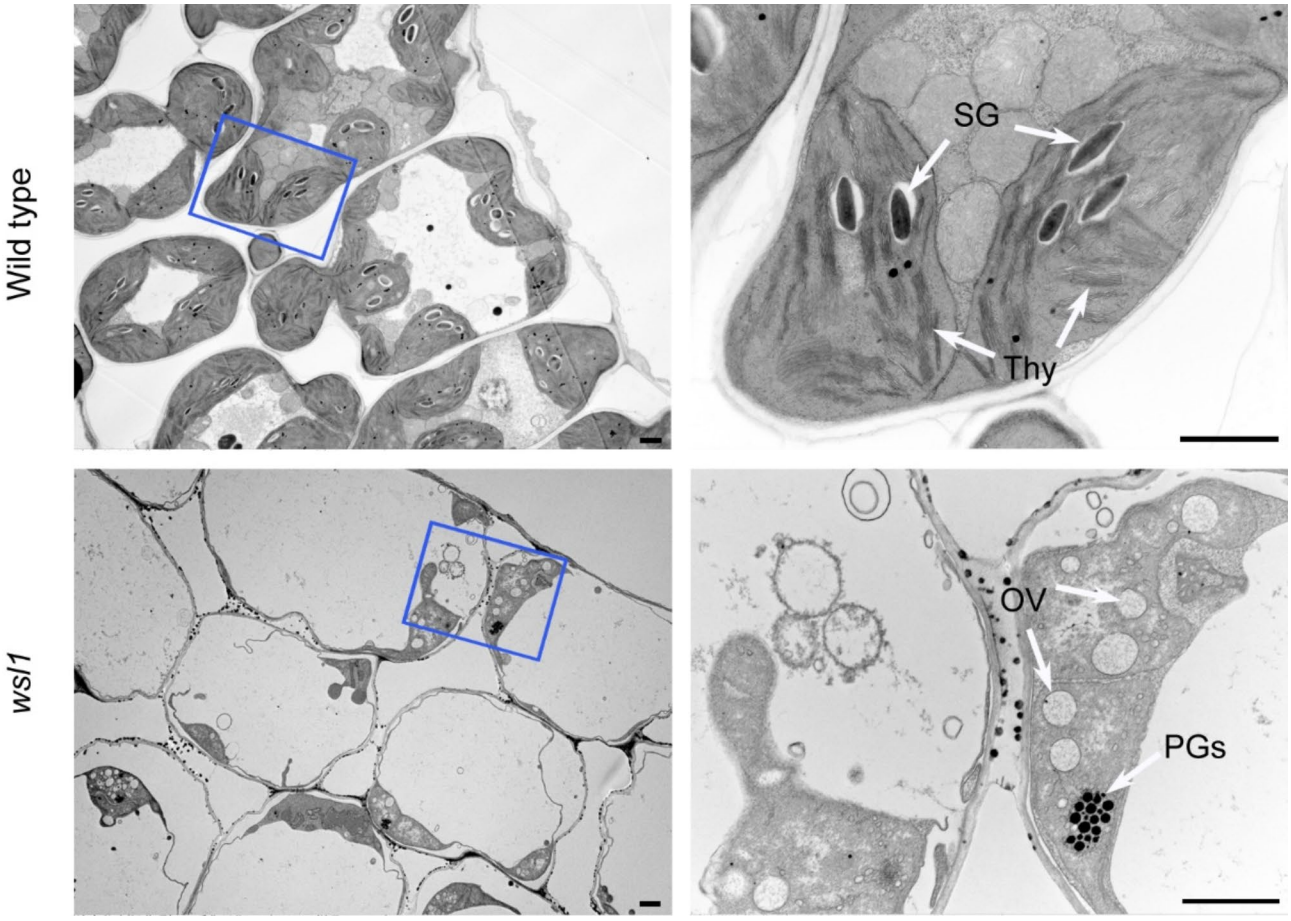

Fig. 2 Transmission electron microscopy images of the leaves of wild-type and *wsl1* plants
Leaves from ten-day-old wild-type and *wsl1* seedlings were used. The right panels are magnifications of the blue boxes in the respective left panels. PGs, plastoglobules. SG, starch granule. Thy, thylakoid. OV, oval-shaped vesicle. Scale bars = 1 μm

two closely related PRDA1 homologs were identified in *Glycine max*, whereas other plant species contained one copy. Multiple sequence alignments revealed that the amino tails of the PRDA1 homologs are hypervariable and that the remaining parts are relatively conserved (Figure S1). Moreover, the deleted amino acids in *wsl1* are conserved among different species and localized in a helix of OsPRDA1 (Fig. 3C, S2).

To verify the biological function of *OsPRDA1*, we used the CRISPR/Cas9 gene editing approach to knock out this gene in wild-type plants. One sequence located in the first exon of *OsPRDA1* was picked as target for gene editing in order to completely abolish the gene function. A 1-bp deletion was detected in the resulting mutant, *OsPRDA1-Cr*, which putatively leads to frame shift and premature termination of protein translation (Fig. 3D, S3). Moreover, the expression level of *OsPRDA1* is significantly downregulated in *OsPRDA1-Cr* (Figure S4). *OsPRDA1-Cr* presented white leaves and eventually died, mimicking the phenotype of *wsl1* (Fig. 3E). Same to *wsl1*, the chloroplast of *OsPRDA1-Cr* also lacks thylakoid membrane and starch granules (Figure S5). Transforming wild-type *OsPRDA1* into *wsl1* rescued the mutant phenotype (Fig. 3E). These results confirmed that the mutant phenotype is indeed caused by *OsPRDA1* dysfunction.

OsPRDA1 Is Located in Chloroplasts

The expression profile of *OsPRDA1* in different organs was determined by qRT-PCR analysis. The results revealed that *OsPRDA1* is highly expressed in leaves and moderately expressed in the internode and panicle. The expression levels of *OsPRDA1* in roots and seeds are relatively low (Fig. 4A). Moreover, *OsPRDA1* transcript levels increased dramatically when dark-grown etiolated seedlings were exposed to light (Fig. 4B).

To examine the subcellular localization of OsPRDA1, we fused OsPRDA1 with green fluorescent protein (GFP) and performed a transient expression assay in rice protoplasts. The results revealed that the green signal of OsPRDA1-GFP overlapped with the chlorophyll autofluorescence signal, whereas the free GFP signal displayed a ubiquitous distribution pattern throughout the

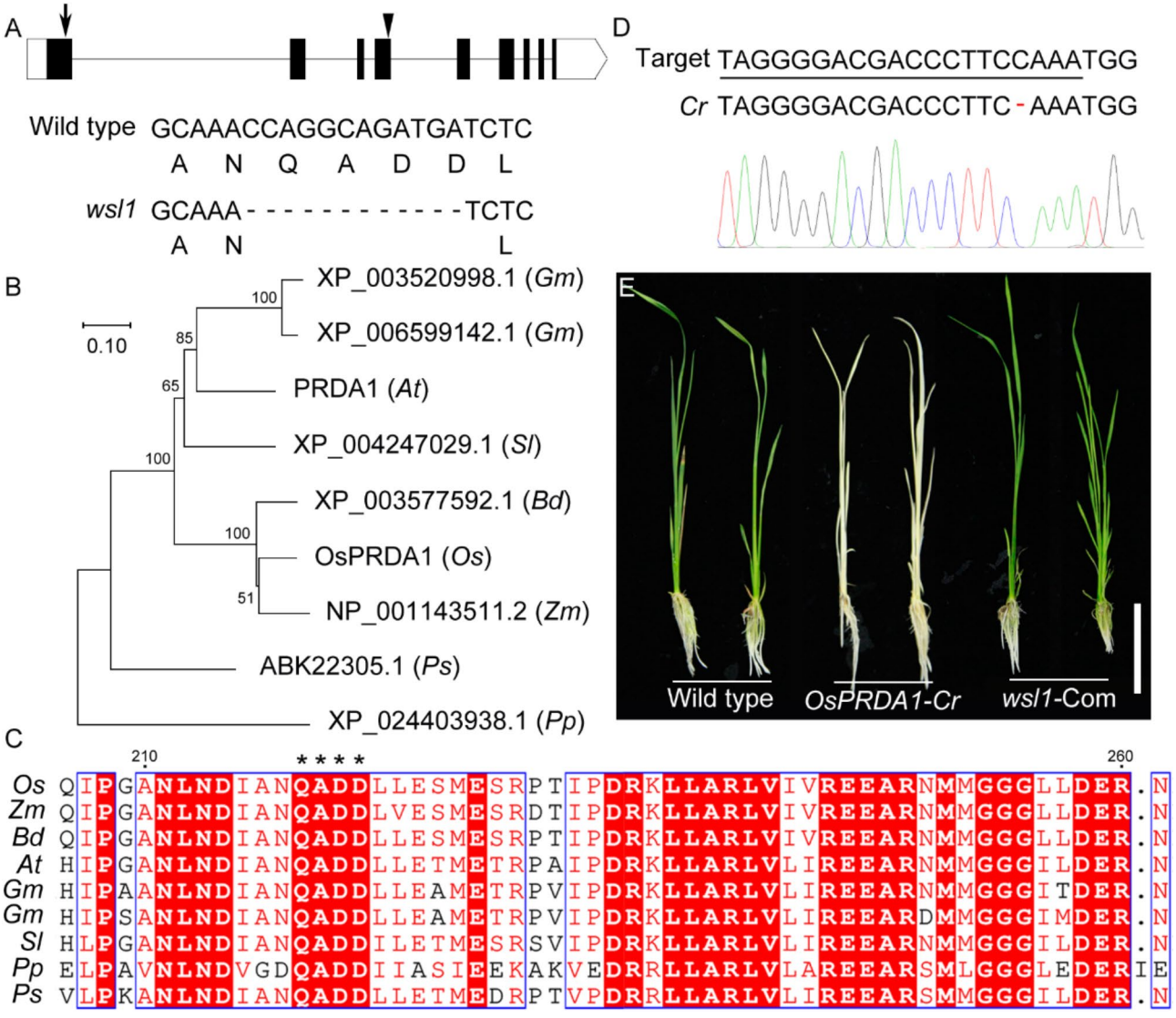

Fig. 3 Characterization and functional verification of *OsPRDA1*
(**A**) Gene structure of *OsPRDA1*. The triangle indicates the position of the mutations in *wsl1*. Details of the sequence modification in *wsl1* are listed below. The arrow indicates the position of the target sequence for gene editing. (**B**) Phylogenetic tree derived from the full-length amino acid sequences of OsPRDA1 homologs in different species. *At*, *Arabidopsis thaliana*. *Bd*, *Brachypodium distachyon*. *Gm*, *Glycine max*. *Os*, *Oryza sativa*. *Pp*, *Physcomitrium patens*. *Ps*, *Picea sitchensis*. *Sl*, *Solanum lycopersicum*. *Zm*, *Zea mays*. (**C**) Multiple sequence alignment of OsPRDA1 homologs spanning the deletion in *wsl1*. The deleted amino acids in *wsl1* are indicated by asterisks. Identical amino acids are shaded in red. (D) Target sequence for CRISPR/Cas9 gene editing and genotypes of knockout mutants (*OsPRDA1-Cr*). (E) Phenotypes of knockout mutants (*OsPRDA1-Cr*) and complemented plants (*wsl1*-Com). Seedlings grown for three weeks were presented. Scale bar = 5 cm

cell (Fig. 4C). These findings indicate that OsPRDA1 is located in chloroplasts, which is consistent with its biological function in chloroplast development.

Genes Related To Photosynthesis Were Differentially Expressed in *wsl1*

To dissect the biological function of OsPRDA1 in chloroplast development, we carried out a transcriptome analysis between the wild type and *wsl1*. Transcriptional profiles of nucleus- and organelle-encoded genes were analyzed and compared. Correlation tests revealed that correlation indices were high among biological replicates and deviated between groups (Fig. 5A). A total of 5,906 genes were differentially expressed in *wsl1* compared with the wild type, including 2,902 upregulated and 3,004 downregulated genes (Fig. 5B). Gene Ontology (GO) analysis revealed that differentially expressed genes (DEGs) were enriched in photosynthesis-related terms, which is in accordance with the albino phenotype of *wsl1* (Fig. 5C). Among the 96 DEGs related to photosynthesis (GO:0015979), 9 nuclear DEGs were upregulated, whereas 73 nuclear and 14 chloroplast

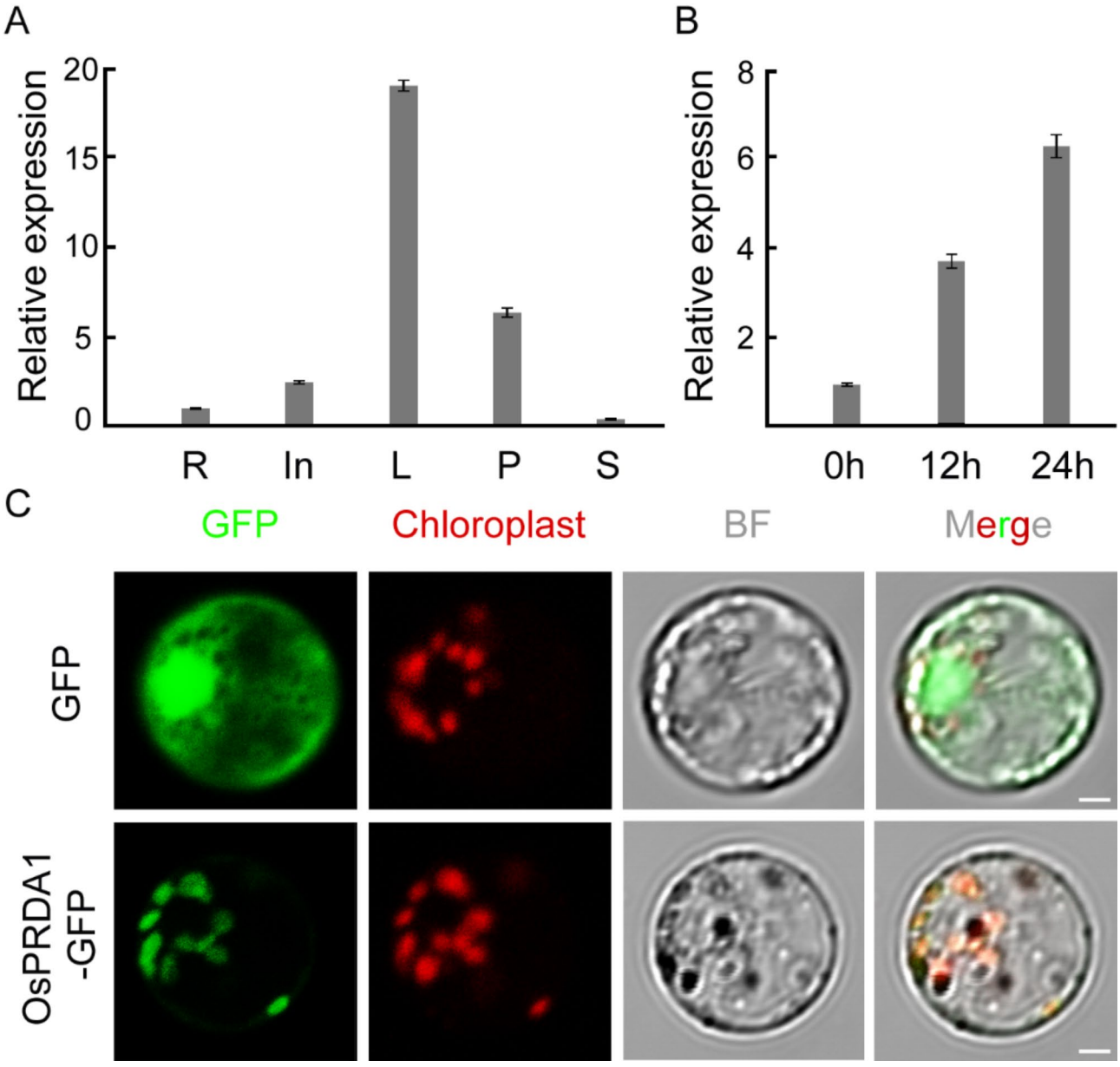

Fig. 4 Expression pattern of *OsPRDA1* and subcellular localization of OsPRDA1
(**A**) qRT-PCR analysis of *OsPRDA1* in different rice tissues. R, root; In, internode; L, leaf; P, panicle; S, seed. Data are presented as the mean ± SD. (**B**) Light-induced expression of *OsPRDA1*. The light exposure times were 12 h and 24 h. Data are presented as the mean ± SD. (**C**) Subcellular localization of OsPRDA1 in rice protoplasts. Green fluorescence indicates the GFP signal, and red fluorescence indicates chloroplast autofluorescence. BF, bright field. Scale bars = 5 μm

DEGs were downregulated. Notably, 56 chloroplast genes were detected in the wild-type and *wsl1* libraries, among which 15 genes were upregulated and 25 genes were downregulated (Fig. 5D). These results suggest that the transcription of photosynthesis-related genes, especially chloroplast genes, are dysregulated in the absence of OsPRDA1.

Downregulated Expression of PEP-dependent Chloroplast Genes in *wsl1*

Plastid genes can be divided into three classes. Class I genes are transcribed by PEPs. Class II genes are transcribed by both PEPs and NEPs. Class III genes are transcribed by NEPs. Previous research has shown that PRDA1 is essentially required for the regulation of PEP-dependent plastid gene expression in *Arabidopsis* (Qiao et al. 2014). To test whether PEP-related genes were altered in *wsl1*, we performed qRT-PCR to analyze and

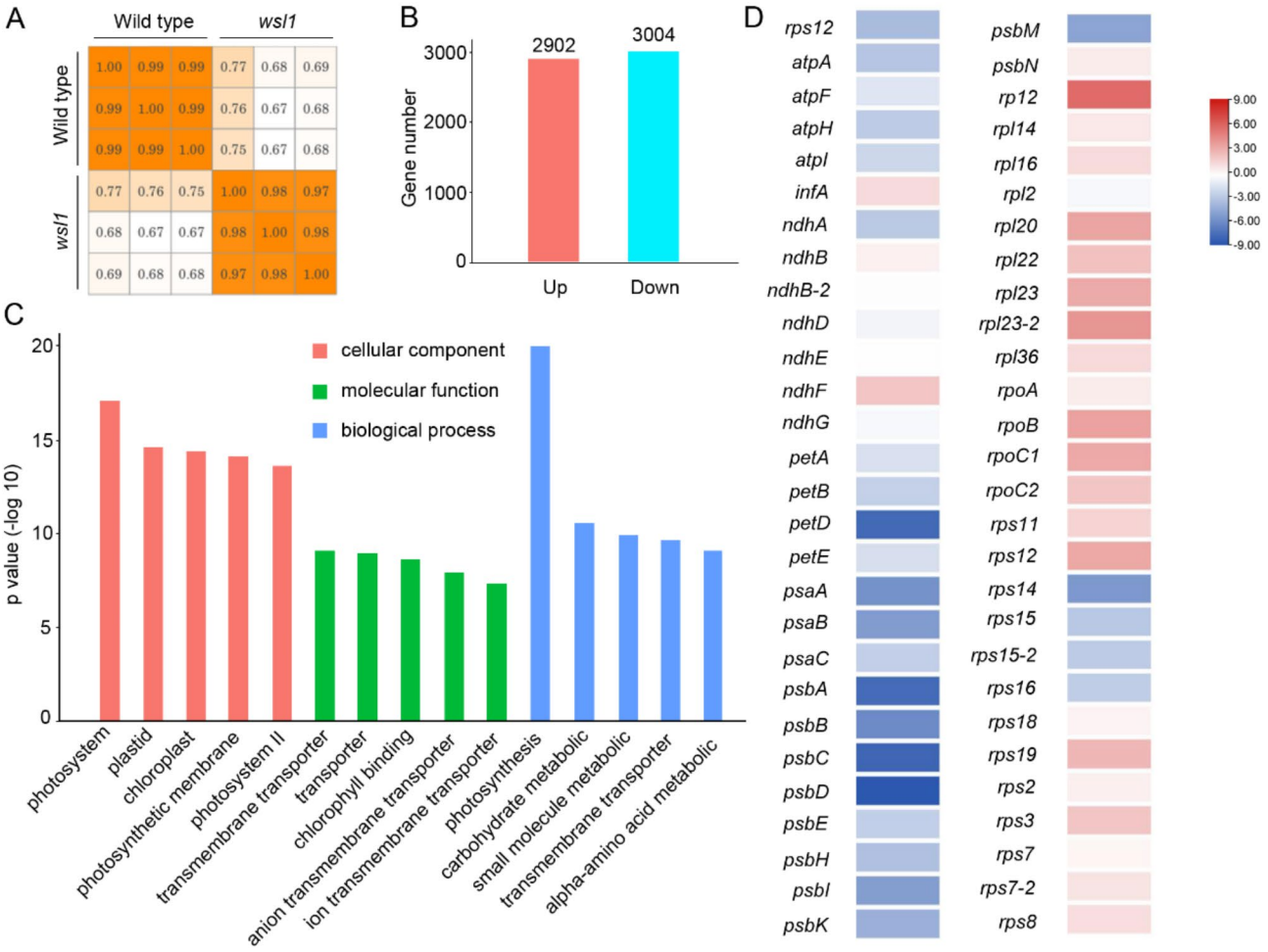

Fig. 5 Transcriptome analysis of the wild type and *wsl1*

(**A**) Correlation of gene expression levels between the wild type and *wsl1*. (**B**) Statistical analysis of differentially expressed genes (DEGs) between the wild type and *wsl1*. (**C**) Gene Ontology (GO) analysis of DEGs, showing the top 5 GO terms in DEGs in *wsl1* relative to the wild type. (**D**) Heatmap of the fold changes (log2) in the expression of chloroplast genes between the wild type and *wsl1*. Data of normalized read counts from transcriptome analysis were used to calculate the expression levels

compare the expression of NEP- and PEP-dependent chloroplast genes between the wild type and *wsl1*. We observed a consistent decrease in the expression levels of PEP-dependent genes (*psbA*, *psbB*, *rbcL*, *psaA*, *psaB*, *petA*, *petB*, *petD*, and *ycf4*) and PEP&NEP-dependent genes (*atpB* and *atpE*) in *wsl1*. The expression level of the NEP-dependent gene, *rpoA* and *rpoB*, increased significantly. Two nuclear-encoded, photosynthesis-related genes, *YGL1* and *DGP1*, were selected for comparison (Wu et al. 2007; Zhang et al. 2021). The expression level of *YGL1* was not significantly different between the wild type and *wsl1*, whereas the expression of *DGP1* was downregulated in *wsl1* (Fig. 6). These results indicated that OsPRDA1 is required for the expression of PEP-dependent plastid genes in rice.

OsFSD2 Interacts With OsPRDA1 and Regulates Chloroplast Gene Expression

Previous research in *Arabidopsis* has shown that PRDA1 interacts with FSD2 (Qiao et al. 2014). To test whether OsPRDA1 also interacts with OsFSD2, we conducted a yeast two-hybrid analysis. The corresponding transformants were subsequently grown on quadruple dropout medium, confirming the interactions between them (Fig. 7A). Since the deleted amino acid of OsPRDA1 in *wsl1* is vital for the protein function, we tested whether they contribute to the interaction with OsFSD2. Yeast two hybrid assay showed that OsPRDA1^{wsl1} also interact with OsFSD2. (Figure S6). As the essential subunit of the PEP complex, FSD2 is required for chloroplast development, and *Arabidopsis fsd2* has a pale green phenotype (Myouga et al. 2008). However, the molecular function of *OsFSD2* (LOC_Os06g02500) has not been elucidated. We used a CRISPR/Cas9 assay to create a mutant of *OsFSD2*

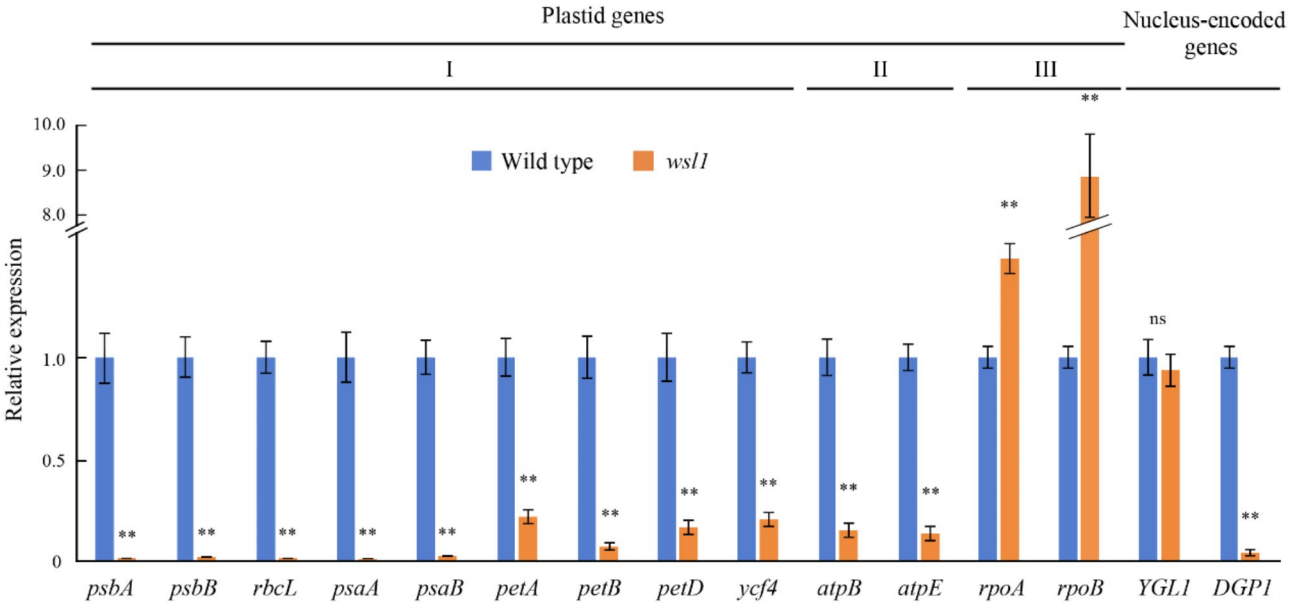

Fig. 6 qRT-PCR analysis of plastid- and nucleus-encoded genes in wild type and *wsl1*
Class I represents PEP-dependent genes; Class II represents PEP- and NEP-dependent genes; and Class III represents NEP-dependent genes. Data are presented as the mean ± SD. Asterisks indicate significant differences according to two-tailed Student's *t* test (**$P < 0.01$). ns, not significant.

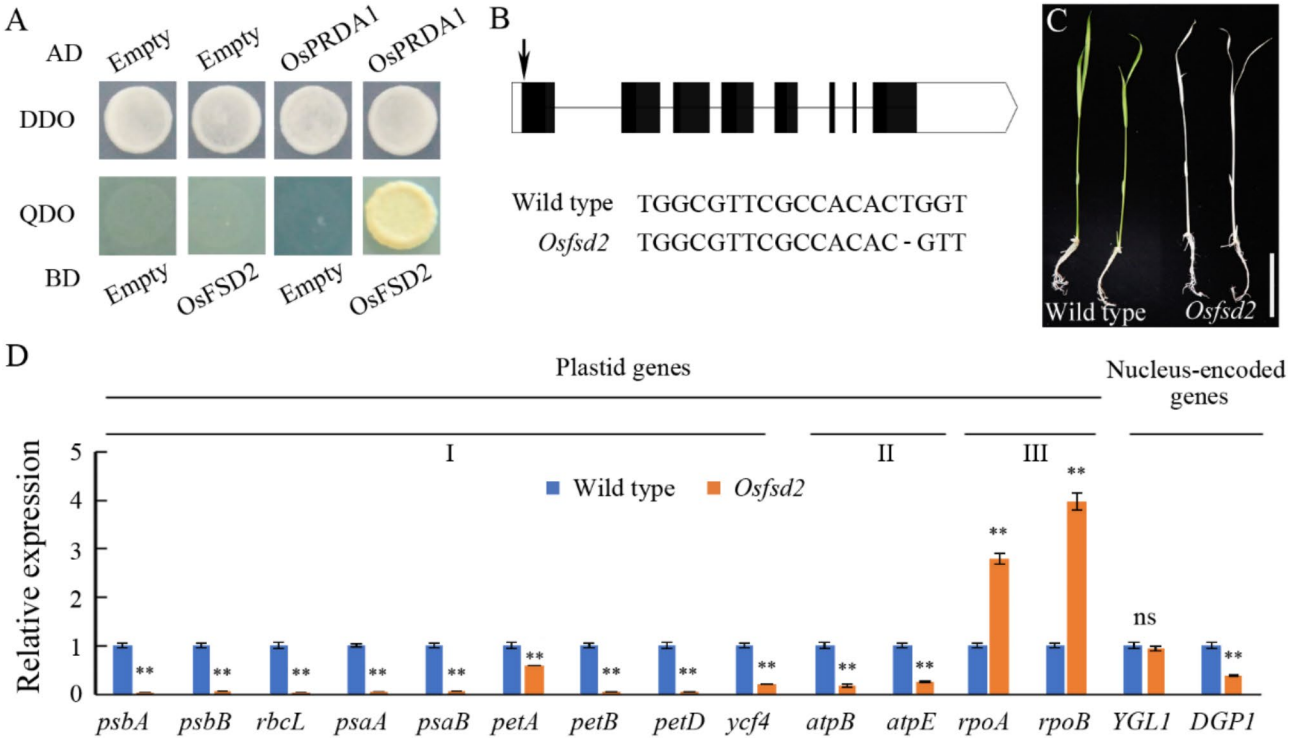

Fig. 7 OsFSD2 interacts with OsPRDA1 and regulates chloroplast gene expression
(**A**) Interaction between OsPRDA1 and OsFSD2 in yeast two-hybrid assays. AD, active domain; BD, binding domain. DDO (SD/-Leu-Trp), double dropout medium. QDO (SD/-His-Leu-Trp-Ade), quadruple dropout medium. (**B**) Gene structure of *OsFSD2*. Coding regions are shown as black boxes. The 5'- and 3'-untranslated regions are shown as white boxes. Introns are shown as black lines. The triangle indicates the position of the target sequence for CRISPR/Cas9. Details of the sequence modifications are listed below. (**C**) Phenotypes of *Osfsd2* knockout mutants. Scale bar = 5 cm. (**D**) qRT-PCR analysis of plastid genes and nucleus-encoded genes in the wild type and *Osfsd2*. Data are presented as the mean ± SD. Asterisks indicate significant differences according to a two-tailed Student's *t* test (**$P < 0.01$). ns, not significant

(Fig. 7B). *Osfsd2* presented white seedlings and eventually died, a phenotype that was more severe than that of *Arabidopsis fsd2* (Fig. 7C). We observed the chloroplast of *Osfsd2* under TEM. The results showed that the chloroplast of *Osfsd2* lacks thylakoid membrane and starch granules, which is similar to that of *wsl1* (Figure S5).

qRT-PCR assay revealed that the expression levels of PEP- and PEP&NEP-dependent genes were decreased significantly in *Osfsd2* and that the expression levels of NEP-dependent genes were increased, which was similar to the findings in *wsl1* (Fig. 7D). These results indicated that OsPRDA1 interacts with OsFSD2 in the regulation of chloroplast gene expression in rice.

Discussion

Dissecting the molecular mechanisms of chloroplast development in crops might pave the way for breeding with high photosynthetic efficiency and production. In this study, we demonstrated the essential role of OsPRDA1 in rice chloroplast development by characterizing a novel rice chlorophyll-deficient mutant, *wsl1* (Fig. 1). Cytological observation by TEM revealed that the chloroplasts of *wsl1* lack thylakoid membranes and starch granules. Instead, oval-shaped vesicles and many densely stained globular structures were present in *wsl1* chloroplasts (Fig. 2). These abnormal suborganelle structures were also observed in *fsd2*, *fsd3*, *ptac6*, *ptac12*, *trx z*, and *ptac7* in *Arabidopsis* (Pfalz et al. 2006; Myouga et al. 2008; Arsova et al. 2010; Yu et al. 2013). These findings indicate that these structures may be derived from a common metabolic defect in plant chloroplasts, although the accurate constitution of these vesicles has been obscure until recently. Mutmap + is reported to be suitable for identifying mutations that cause early development lethality, sterility, and other defects that generally hinder crossing (Fekih et al. 2013). This approach was adopted to isolate the causal gene, which was named *OsPRDA1* because of its homology with *PRDA1* in *Arabidopsis* (Qiao et al. 2014). Knockout of *PRDA1* in *Arabidopsis* caused a seedling-lethal, albino phenotype and arrested the development of leaf chloroplasts, which is similar to the phenotype of *wsl1*. OsPRDA1 is located in chloroplasts, which is consistent with its function in chloroplast development (Fig. 4C).

Transcriptome analysis revealed that photosynthesis-related genes, especially chloroplast genes, were enriched in DEGs between the wild type and *wsl1* (Fig. 5). Importantly, the expression levels of the examined PEP-dependent chloroplast genes were downregulated in *wsl1* (Fig. 6). We proved that OsPRDA1 interacts with OsFSD2, a member of PEP-associated proteins (PAPs). However, the biological function of rice FSD2 in chloroplast development has not been determined. We knocked out the *OsFSD2* gene and observed an albino and seedling-lethal phenotype. PEP-dependent chloroplast genes were downregulated in *Osfsd2* (Fig. 7). These results suggested that *OsPRDA1* and *OsFSD2* may function in the same biological pathway in rice chloroplast development.

Recently, the cryo-EM structures of *Nicotiana tabacum* (tobacco) chloroplast RNA polymerase apoenzyme and transcription elongation complexes revealed the composition, assembly, function, and evolution of the chloroplast transcription apparatus (Wu et al. 2024). Fifteen PAPs bind at the periphery of the PEP core and facilitate assembly of the PEP-PAP supercomplex. Among them, the protection module consists of two Fe-SOD enzymes that form a heterodimer (PAP4 and PAP9; also named FSD3 and FSD2, respectively). Transgenic *Arabidopsis* plants overexpressing both the *FSD2* and *FSD3* genes presented increased tolerance to oxidative stress. FSD2 and FSD3 have been proposed to act as ROS scavengers in the maintenance of early chloroplast development by protecting the chloroplast nucleoids from ROS (Myouga et al. 2008). Similarly, the accumulation of O_2^- in dark-acclimated *PRDA1*-deficient plants was significantly greater than that in wild-type control plants but was similar to that in *fsd2* plants (Qiao et al. 2014). Nitro blue tetrazolium (NBT) staining was used to measure the content of superoxide anion radicals (O_2^-). *wsl1* and *Osfsd2* were stained deeper than the wild type, indicating that more superoxide radicals accumulated (Figure S7). However, further studies are needed to test whether OsPRDA1 also functions in maintaining the redox state around chloroplast nucleoids.

Manipulating the expression levels of PAP-encoding genes may promote plant development and resistance to stress. OsFSD2 was reported to positively regulate chilling tolerance in rice, as the overexpression of *OsFSD2* resulted in improved chilling tolerance, and the phenotypes of the *OsFSD2-RNAi* lines were opposite those of the *OsFSD2-OE* lines (Ge et al. 2020). The overexpression of *ALM1*/*OsFSD3* increased SOD enzyme activity, leading to increased scavenging of superoxide anion radicals and conferring drought stress in rice seedlings (Wang et al. 2021b). *OsPAP3* overexpression increased the number of chloroplasts and improved rice grain yield by approximately 25%, largely through increased tiller formation (Seo et al. 2024). Thus, it is tempting to test whether manipulation of the *OsPRDA1* expression level (e.g., overexpression) could promote rice development and be applied to create rice with improved growth and productivity.

Conclusions

OsPRDA1 interacts with OsFSD2, a member of PAPs. Mutation of *OsPRDA1* and *OsFSD2* leads to misregulation of PEP-dependent chloroplast genes and defects in

chloroplast development. These results will facilitate efforts to further elucidate the molecular mechanism of chloroplast gene expression in rice.

Materials and methods

Plant Materials

The *wsl1* mutant was isolated from a collection of mutants from our laboratory, which were induced by ^{60}Co γ-ray irradiation of the *japonica* rice (*Oryza sativa*) variety Yandao 8. The Yandao 8 variety was used as the wild type in all the experiments. The plant materials were cultivated in an experimental plot in an incubator. The photoperiod of the incubator was 14 h in light, with 20,000 lx, and 10 h in the dark.

Measurement of Pigment Contents

Pigment contents were determined using a previously described method with slight modifications (Zhang et al. 2021). Fresh leaves (0.1 g) were cut and soaked in a 10 ml solution of 1:1 ethanol: acetone (v/v). After 12 h of treatment in darkness, the absorbance values at 470, 649, and 665 nm wavelengths were measured using a microplate reader. The pigment contents were calculated based on the absorbance values. All experiments were carried out with three biological replicates.

Transmission electron Microscopy Analysis

Fresh leaves of the wild type, *wsl1*, *OsPRDA1-Cr*, and *Osfsd2* were cut into pieces and fixed in 3% glutaraldehyde in phosphate buffer. After washing with phosphate buffer (0.1 M) three times, the samples were fixed in 1% OsO4 for 1.5 h. After fixation, the samples were washed again in phosphate buffer (0.1 M) three times. The samples were dehydrated through an acetone series (50% for 15 min, 70% for 15 min, 90% for 15 min, 100% for 20 min, 20 min, and 20 min) and ultimately embedded in Epon812 resin (acetone: embedding fluid = 2:1 for 0.5 h, acetone: embedding fluid = 1:2 for 1.5 h at 37 ℃, embedding fluid for 3 h at 37 ℃). After solidifying at 37 ℃, 45 ℃, and 60 ℃ for 24 h, ultrathin Sect. (70 nm) were produced using an LKB-V slicer. The samples were double stained with uranyl acetate and lead citrate for 15 min, respectively. The sections were then observed with a JEOL-1200E transmission electron microscope and documented by MORADA-G2.

Mutmap+

Briefly, the genomic DNA of 38 wild-type progenies and 38 mutant-type progenies in the M3 segregating population were mixed and sequenced to produce 19.03× and 19.59× average sequence depths. Mapping the reads to the reference genome (*Oryza sativa* Japonica Group cultivar, *Nipponbare*) identified 343,777 mutation sites. The mutation index of identified mutation sites, including the intrinsic sequence variation between the background and reference genomes, was obtained by calculating the ratio between the number of reads with corresponding mutations and the total number of reads spanning this site. Mutation sites were filtered by the following criteria: (1) the mutation index of the mutant bulk was 1, as the phenotype was unambiguous; (2) the mutation index of the wild-type bulk was < 0.5, as it contained the wild type, with a mutation index = 0, and heterozygotes, with an expected mutation index = 0.5.

Gene Editing and Complementary Assay

The CRISPR/Cas9 gene editing approach in rice was performed according to a protocol described previously (Ma et al. 2015). Briefly, the target sequence was designed using CRISPR-GE, a convenient software toolkit for CRISPR-based genome editing (http://skl.scau.edu.cn/). The OsU6a promoter, target sequence, and gRNA were linked through two rounds of PCR. In the first round of PCR, the target sequence was linked to the OsU6a promoter and gRNA using specifically designed primers. In the second round of PCR, mixed DNA from the first PCR, both of which harbored overlapping target sequences, was used as a template to link the three elements. The PCR products were subsequently cloned and inserted into the pYLCRISPR/Cas9-MH vector by *Bsa* I digestion and T4 ligation. The resulting constructs were sequenced and transformed into *Agrobacterium tumefaciens* EHA105 and then into calli of Yandao 8, a japonica variety. T0 plants were genotyped to obtain the mutants.

For the complementary assay, the CDS of *OsPRDA1* was inserted into the pCAMBIA23A vector with the rice actin promoter. The transgene procedures used were the same as those used for gene editing. Complemented plants were characterized by mutation of endogenous *OsPRDA1* and transgenic positivity.

qRT–PCR Assay

Total RNA was extracted from rice tissues using TRIzol reagent. Reverse transcription was performed using HiScript III RT SuperMix for RT−qPCR (+ gDNA wiper; Vazyme). Real-time PCR analysis was performed using ChamQ SYBR qPCR Master Mix (Vazyme) and a Bio-Rad CFX96 real-time PCR instrument. All the PCR experiments were conducted using 40 cycles of 95 ℃ for 10 s and 60 ℃ for 30 s. All the reactions were performed in triplicate, with *ubiquitin* as the normalized reference gene for all the comparisons. The primers used for qRT−PCR are listed in Table S1.

Subcellular Localization of OsPRDA1

The coding sequence of *OsPRDA1* was amplified, cloned, and inserted into the pJIT163-GFP vector (Biovector, Beijing, China) in frame with GFP. The resulting plasmids

were subsequently transfected into rice protoplasts through PEG-mediated transformation. Empty pJIT163-GFP vector was used as the control. Fluorescence signals were captured at 24 h after transformation with a confocal laser scanning microscope (Carl Zeiss LSM 710, Oberkochen, Germany). GFP and red fluorescence signals (chloroplast autofluorescence) were excited at 488 and 561 nm, and emissions were collected at 500–540 nm and 600–650 nm, respectively. The primers used for PCR are listed in Table S1.

RNA-seq

Total RNA was extracted from wild-type and *wsl1* leaves at 14 DAG (Invitrogen Life Technologies). The RNA sequencing libraries were prepared from 2 μg of total RNA with the following modifications. Ribosomal RNA was removed using an Epicentre Ribo-Zero™ rRNA Removal Kit. Using RNA as a template and random oligonucleotides as primers, the first strand of cDNA was synthesized, and then, RNase H was used to degrade the RNA strand. To select cDNA fragments of the preferred 400–500 bp in length, the library fragments were purified using the AMPure XP system (Beckman Coulter, Beverly, CA, USA). The sequencing library was then sequenced on a NovaSeq 6000 platform (Illumina) and analyzed.

NBT Staining

Leaves were excised and placed in NBT solution for 4 h under room temperature. Vacuum the sample (-0.1 MPa, 0.5 h) for better penetration. Samples were immersed in 95% ethanol for decolorization at 65 ℃. After cooling, NBT-treated leaves were examined under the light microscope and photographed.

Computational Sequence Analysis

The protein sequences of the OsPRDA1 homologs were blasted and downloaded from NCBI. The phylogenetic tree was constructed in MegaX using the neighbor-joining method. The bootstrap method with 1000 replications was used in the construction of the phylogeny. The Poisson model was adopted for substitutions. The pairwise deletion option was applied. Multiple sequence alignment was conducted using MAFFT (https://toolkit.tuebingen.mpg.de/#/tools/mafft) and colored with ESPript (http://espript.ibcp.fr/ESPript/ESPript/). The 3D structure was predicted by SWISS-MODEL (https://swissmodel.expasy.org/interactive).

Supplementary Information

The online version contains supplementary material available at https://doi.org/10.1186/s12284-025-00771-x.

Supplementary Material 1

Supplementary Material 2

Author Contributions

H.Y. conceived the project. C.Z. conducted the majority of the experiments. L.W., Z.W., Q.D., H.F., S.X., X.L., and J.T. helped with the construction of some materials and cytological observations. C.Z. wrote the manuscript under the supervision of H.Y.

Funding

This work was supported by the Biological Breeding-National Science and Technology Major Project (2023ZD04068), the Zhongshan Laboratory of Biological Breeding (ZSBBL-KY2023-06), the National Natural Science Foundation of China (32200690, 32370901), the Postdoctoral Research Funding Program of Jiangsu Province (2021K057A), and the Jiangsu Higher Education Institutions of China (PAPD).

Data Availability

All the data generated or analyzed during this study are included in this published article and its supplementary information files.

Declarations

Ethics Approval and Consent to Participate

Not applicable.

Consent for Publication

Not applicable.

Competing Interests

The authors declare no competing interests.

Received: 29 October 2024 / Accepted: 2 March 2025
Published online: 12 March 2025

References

Arsova B, Hoja U, Wimmelbacher M, Greiner E, Üstün S, Melzer M, Petersen K, Lein W, Börnke F (2010) Plastidial thioredoxin interacts with two Fructokinase-Like proteins in a Thiol-Dependent manner: evidence for an essential role in Chloroplast development in *Arabidopsis* and *Nicotiana benthamiana*. Plant Cell 22:1498–1515

Börner T, Aleynikova AY, Zubo YO, Kusnetsov VV (2015) Chloroplast RNA polymerases: role in Chloroplast biogenesis. Biochim Et Biophys Acta-Bioenergetics 1847:761–769

Daniell H, Jin SX, Zhu XG, Gitzendanner MA, Soltis DE, Soltis PS (2021) Green giant-a tiny Chloroplast genome with mighty power to produce high-value proteins: history and phylogeny. Plant Biotechnol J 19:430–447

Díaz MG, Hernández-Verdeja T, Kremnev D, Crawford T, Dubreuil C, Strand Å (2018) Redox regulation of PEP activity during seedling establishment in *Arabidopsis thaliana*. Nat Commun 9:50

Fekih R, Takagi H, Tamiru M, Abe A, Natsume S, Yaegashi H, Sharma S, Sharma S, Kanzaki H, Matsumura H, Saitoh H, Mitsuoka C, Utsushi H, Uemura A, Kanzaki E, Kosugi S, Yoshida K, Cano L, Kamoun S, Terauchi R (2013) MutMap+: genetic mapping and mutant identification without crossing in rice. PLoS ONE 8:e68529

Garcia M, Myouga F, Takechi K, Sato H, Nabeshima K, Nagata N, Takio S, Shinozaki K, Takano H (2008) An homolog of the bacterial peptidoglycan synthesis enzyme mure has an essential role in Chloroplast development. Plant J 53:924–934

Ge Q, Zhang YY, Xu YY, Bai MY, Luo W, Wang B, Niu YD, Zhao Y, Li SS, Weng YX, Wang ZY, Qian Q, Chong K (2020) Cyclophilin OsCYP20-2 with a novel variant integrates defense and cell elongation for chilling response in rice. New Phytol 225:2453–2467

Gilkerson J, Perez-Ruiz JM, Chory J, Callis J (2012) The plastid-localized pfkB-type carbohydrate kinases FRUCTOKINASE-LIKE 1 and 2 are essential for growth and development of *Arabidopsis thaliana*. BMC Plant Biol 12:102

He L, Zhang S, Qiu ZN, Zhao J, Nie WD, Lin HY, Zhu ZG, Zeng DL, Qian Q, Zhu L (2018) FRUCTOKINASE-LIKE PROTEIN 1 interacts with TRXz to regulate Chloroplast development in rice. J Integr Plant Biol 60:94–111

Hedtke B, Börner T, Weihe A (2000) One RNA polymerase serving two genomes. EMBO Rep 1:435–440

Kindgren P, Kremnev D, Blanco NE, Lopez JDB, Fernández AP, Tellgren-Roth C, Kleine T, Small I, Strand Å (2012) The *plastid redox insensitive 2* mutant of *Arabidopsis* is impaired in PEP activity and high light-dependent plastid redox signalling to the nucleus. Plant J 70:366–366

Lin DZ, Zheng KL, Liu ZH, Li ZK, Teng S, Xu JL, Dong YJ (2018) Rice *TCM1* encoding a component of the TAC complex is required for Chloroplast development under cold stress. Plant Genome 11:1

Lv YS, Shao GN, Qiu JH, Jiao GA, Sheng ZH, Xie LH, Wu YW, Tang SQ, Wei XJ, Hu PS (2017) White leaf and panicle 2, encoding a PEP-associated protein, is required for Chloroplast biogenesis under heat stress in rice. J Exp Bot 68:5147–5160

Ma X, Zhang Q, Zhu Q, Liu W, Chen Y, Qiu R, Wang B, Yang Z, Li H, Lin Y, Xie Y, Shen R, Chen S, Wang Z, Chen Y, Guo J, Chen L, Zhao X, Dong Z, Liu YG (2015) A robust CRISPR/Cas9 system for convenient, High-Efficiency multiplex genome editing in monocot and Dicot plants. Mol Plant 8:1274–1284

Martin W, Stoebe B, Goremykin V, Hapsmann S, Hasegawa M, Kowallik KV (1998) Gene transfer to the nucleus and the evolution of chloroplasts. Nature 393:162–165

Myouga F, Hosoda C, Umezawa T, Iizumi H, Kuromori T, Motohashi R, Shono Y, Nagata N, Ikeuchi M, Shinozaki K (2008) A heterocomplex of Iron superoxide dismutases defends Chloroplast nucleoids against oxidative stress and is essential for Chloroplast development in *Arabidopsis*. Plant Cell 20:3148–3162

Pfalz J, Liere K, Kandlbinder A, Dietz KJ, Oelmüller R (2006) pTAC2,-6, and-12 are components of the transcriptionally active plastid chromosome that are required for plastid gene expression. Plant Cell 18:176–197

Pfannschmidt T, Blanvillain R, Merendino L, Courtois F, Chevalier F, Liebers M, Grübler B, Hommel E, Lerbs-Mache S (2015) Plastid RNA polymerases: orchestration of enzymes with different evolutionary origins controls Chloroplast biogenesis during the plant life cycle. J Exp Bot 66:6957–6973

Qiao JW, Ma CL, Wimmelbacher M, Börnke F, Luo MZ (2011) Two novel proteins, MRL7 and its paralog MRL7-L, have essential but functionally distinct roles in Chloroplast development and are involved in plastid gene expression regulation in *Arabidopsis*. Plant Cell Physiol 52:1017–1030

Qiao JW, Li J, Chu W, Luo MZ (2014) PRDA1, a novel Chloroplast nucleoid protein, is required for early Chloroplast development and is involved in the regulation of plastid gene expression in *Arabidopsis*. Plant Cell Physiol 55:467–467

Qiu ZN, Kang SJ, He L, Zhao J, Zhang S, Hu J, Zeng DL, Zhang GG, Dong GJ, Gao ZY, Ren DY, Chen G, Guo LB, Qian Q, Zhu L (2018) The newly identified gene affects Chloroplast development in rice. Plant Sci 267:168–179

Seo DH, Jang J, Park D, Yoon Y, Choi YD, Jang G (2024) PEP-ASSOCIATED PROTEIN 3 regulates rice tiller formation and grain yield by controlling Chloroplast biogenesis. Plant Physiol 194:805–818

Steiner S, Schröter Y, Pfalz J, Pfannschmidt T (2011) Identification of essential subunits in the plastid-Encoded RNA polymerase complex reveals Building blocks for proper plastid development. Plant Physiol 157:1043–1055

Swiatecka-Hagenbruch M, Emanuel C, Hedtke B, Liere K, Börner T (2008) Impaired function of the phage-type RNA polymerase RpoTp in transcription of Chloroplast genes is compensated by a second phage-type RNA polymerase. Nucleic Acids Res 36:785–792

Wang DK, Liu HQ, Zhai GW, Wang LS, Shao JF, Tao YZ (2016a) *OspTAC2* encodes a pentatricopeptide repeat protein and regulates rice Chloroplast development. J Genet Genomics 43:601–608

Wang LW, Wang CM, Wang YH, Niu M, Ren YL, Zhou KN, Zhang H, Lin QB, Wu FQ, Cheng ZJ, Wang JL, Zhang X, Guo XP, Jiang L, Lei CL, Wang J, Zhu SS, Zhao ZC, Wan JM (2016b) WSL3, a component of the plastid-encoded plastid RNA polymerase, is essential for early Chloroplast development in rice. Plant Mol Biol 92:581–595

Wang YL, Wang YH, Ren YL, Duan EC, Zhu XP, Hao YY, Zhu JP, Chen RB, Lei J, Teng X, Zhang YY, Wang D, Zhang X, Guo XP, Jiang L, Liu SJ, Tian YL, Liu X, Chen LM, Wang HY, Wan JM (2021a) *WHITE PANICLE2* encoding thioredoxin, regulates plastid RNA editing by interacting with multiple organellar RNA editing factors in rice. New Phytol 229:2693–2706

Wang YW, Deng C, Ai PF, Cui XA, Zhang ZG (2021b) *ALM1*, encoding a Fe-superoxide dismutase, is critical for rice Chloroplast biogenesis and drought stress response. Crop J 9:1018–1029

Wu ZM, Zhang X, He B, Diao LP, Sheng SL, Wang JL, Guo XP, Su N, Wang LF, Jiang L, Wang CM, Zhai HQ, Wan JM (2007) A chlorophyll-deficient rice mutant with impaired chlorophyllide esterification in chlorophyll biosynthesis. Plant Physiol 145:29–40

Wu XX, Mu WH, Li F, Sun SY, Cui CJ, Kim C, Zhou F, Zhang Y (2024) Cryo-EM structures of the plant plastid-encoded RNA polymerase. Cell 187:1127–1144

Yagi Y, Ishizaki Y, Nakahira Y, Tozawa Y, Shiina T (2012) Eukaryotic-type plastid nucleoid protein pTAC3 is essential for transcription by the bacterial-type plastid RNA polymerase. Proc Natl Acad Sci USA 109:7541–7546

Yu QB, Lu Y, Ma Q, Zhao TT, Huang C, Zhao HF, Zhang XL, Lv RH, Yang ZN (2013) TAC7, an essential component of the plastid transcriptionally active chromosome complex, interacts with FLN1, TAC10, TAC12 and TAC14 to regulate Chloroplast gene expression in *Arabidopsis thaliana*. Physiol Plant 148:408–421

Yu QB, Huang C, Yang ZN (2014a) Nuclear-encoded factors associated with the Chloroplast transcription machinery of higher plants. Front Plant Sci 5:316

Yu QB, Ma Q, Kong MM, Zhao TT, Zhang XL, Zhou Q, Huang C, Chong K, Yang ZN (2014b) AtECB1/MRL7, a Thioredoxin-Like fold protein with disulfide reductase activity, regulates Chloroplast gene expression and Chloroplast biogenesis in *Arabidopsis thaliana*. Mol Plant 7:206–217

Zhang C, Zhang JX, Tang YJ, Liu KW, Liu Y, Tang JQ, Zhang T, Yu HX (2021) DEEP GREEN PANICLE1 suppresses GOLDEN2-LIKE activity to reduce chlorophyll synthesis in rice glumes. Plant Physiol 185:469–477

Zhang C, Mao XC, Feng XX, Sun YL, Wang ZR, Tang JQ, Yu HX (2023) OsALB3 is required for Chloroplast development by promoting the accumulation of Light-Harvesting Chlorophyll-Binding proteins in rice. Plants-Basel 12:4003

Zhelyazkova P, Sharma CM, Förstner KU, Liere K, Vogel J, Börner T (2012) The primary transcriptome of barley chloroplasts: numerous noncoding RNAs and the dominating role of the Plastid-Encoded RNA polymerase. Plant Cell 24:123–136

Publisher's Note